

# Local phenomena around a steel dowel embedded in a stone masonry wall

R. Felicetti<sup>1</sup>, N. Gattesco<sup>1</sup> and E. Giuriani<sup>2</sup>

(1) Dipartimento di Ingegneria Civile, Università degli Studi di Udine, via Delle Scienze, 208, 33100 Udine, Italy.

(2) Dipartimento di Ingegneria Civile, Università degli Studi di Brescia, via Branze, 38, 25123 Brescia, Italy.

## ABSTRACT

The study of the local behaviour of steel dowels used to transfer horizontal shear loads between concrete slabs and stone masonry walls has been carried out. Monotonic loading tests have been performed on six specimens of stone masonry made in the laboratory concerning three different embedding techniques for dowels. The geometric interferometry technique was adopted to survey the surface displacements, in the load direction, of the loaded stone block and surrounding mortar joints. For applying the shear load to the connection, a special experimental apparatus has been designed so as to allow the arrangement of moiré gratings as well as to capture the sequence of the fringe pattern.

## RÉSUMÉ

On présente une étude du comportement local des goujons en acier utilisés pour transférer les charges horizontales de cisaillement entre une dalle en béton armé et un mur en pierre. Des essais permettant d'augmenter la charge de façon monotone ont été réalisés sur six échantillons de mur en pierre fabriqués en laboratoire; trois techniques différentes d'ancrage des goujons ont été étudiées. La technique d'interférométrie géométrique a été employée pour étudier les déplacements en surface, dans la direction de la charge, du bloc de pierre chargée et des joints de mortier l'entourant. Afin d'appliquer une charge horizontale à la connexion, un appareil expérimental spécial a été réalisé pour permettre le positionnement d'une grille moiré et de saisir la séquence des franges.

## NOTATION

$s$	slip of the load device with respect to the undisturbed masonry wall
$\eta_d$	displacement of the steel dowel on the surface of the wall with respect to the undisturbed masonry wall
$\eta_s$	displacement of the loaded stone block with respect to the undisturbed masonry wall
$F$	shear load
$\phi$	steel rod diameter
$l_1, l_2$	lever arms of load machine
$e, b$	geometrical parameters of the load device.

## 1. INTRODUCTION

The seismic behaviour of ancient buildings is considerably influenced by the distribution of masses, which are mainly located in the thick masonry walls. Hence, when the seismic action takes effect perpendicularly to the walls, out-of-plane failure can occur if the existing floors (usually wooden floors) are not able to restrain the walls. Therefore, stiff diaphragms are needed at each

floor and they must be well-connected to the walls in order to give a global box behaviour to the building [1].

Very often, these diaphragms are obtained by means of a thin reinforced concrete slab which is overlaid onto the existing wooden floor [2]. This technique was also proposed to improve the flexural stiffness because a composite wood-to-concrete section is obtained with adequate connection devices [3].

With regard to the seismic behaviour, the concrete slab has to be able to restrain the walls against the out-of-plane forces (tie effect) and to transfer the seismic horizontal actions to the shear resistant walls (shear effect).

Usually, concrete dovetail elements, which are embedded in the masonry, are adopted to connect the slab boundary tie-beams to the walls. However, the formation of dovetail niches in the masonry can damage and weaken the surrounding part of the wall. Moreover, this cannot be proposed for historic buildings, especially when artistic and decorated facades have to be preserved. In such cases, connection techniques which limit the damage in the masonry are preferred.

This goal can be reached using distributed steel rods anchored into small drilled holes made in the masonry stone blocks or bricks.

A lot of care is needed to fasten the steel rods in order to assure the effectiveness against tensile action. In practice, steel plates placed on the outer face of the wall can be welded to the rods which pass through the entire wall thickness [4]. When the preservation of the building facade is required, the steel bars can be bonded by means of epoxy resin or grouted cement injected in a blind hole not much larger than the bar diameter [1,5]. However, only a few connectors are usually needed to resist pull-out forces because of their high strength and stiffness.

With respect to the shear resistance of the connection, a great contribution is made by the interlocking effect between the concrete slab and the masonry wall, when the confining action produced by the tie bars is effective. However, the progressive damage at the slab-wall interface caused by cyclic loads may reduce this contribution to zero after a few cycles, and the residual resource in shear transfer depends on the dowel behaviour of the steel rods [4]. The dowel mechanism is considerably weaker than that related to the interlocking effect, and then several connectors are required to maintain the effectiveness of the connection.

In practice, simple fasten techniques are preferable in order to reduce the cost of the intervention. A particular connection technique which does not employ any injected material has been proposed in [6]. The steel rod is forced into a hole which is drilled in a single stone block of adequate size ( $> 15$  cm). Three thin steel strips are then introduced into the hole before dowel insertion to eliminate the clearance and provide a controlled pressure along the rod-hole interface.

The experimental tests carried out on the stone masonry wall of an ancient building [6] provided information on the relationship between the shear load and the deformation of the connection. In particular, an almost bilinear relationship has been obtained, which is characterised by a sudden decrease of stiffness after the bar yielding. No significant loss of bearing capacity occurred after the splitting of the stone, and no macroscopic damage to the masonry texture was observed up to the maximum slip applied (10 mm). Some local phenomena did occur, like the separation of a half-cone-shaped splinter from the surface of the stone and the local settlement of the mortar layer compressed by the stone block.

The experimental investigation on these local phenomena becomes important, especially in the expectation of further theoretical modelling, and concerns the aim of the present research work. Particular attention is paid both to the study of the stress diffusion close to the bar and to the stone movement in the masonry. Specific shear tests have been carried out using the geometric interferometry method (moiré) [7-9] to obtain the field of deformations on the masonry surface around the dowel and the stone block.

## 2. TEST SPECIMENS

The present research work concerns a particular kind of masonry wall which is quite common in some countries and is made with cobblestones of limestone, sandstone, dolomite, etc. The majority of these rounded

stone units have a limited size, ranging between 15 and 20 cm, and are assembled very carefully with some rubble in order to avoid overly-thick joints ( $< 2$  cm).

The mortar used for the joints is made with silica sand and hydrated lime as binder, and it generally has a very low compressive strength (0.25–2.5 MPa).

The horizontal shear transfer between the concrete slab and the masonry wall can be effectively obtained by means of dowel connectors anchored in single stone blocks. Three different anchorage techniques have been studied herein.

In the first technique (type A), the steel rod (16 mm diameter, 352 MPa yielding stress) is forced into a drilled hole having the same diameter as the rod and a depth of about ten times the rod diameter (Fig. 1a). Some difficulties in obtaining a calibrated hole could provoke loss of effectiveness of the connection because the rod can remain slack in its seat or split the stone block during the insertion.

These problems are avoided in the case of technique B. The steel rod is forced into a slightly larger hole (18 mm) drilled in a single stone block where three steel

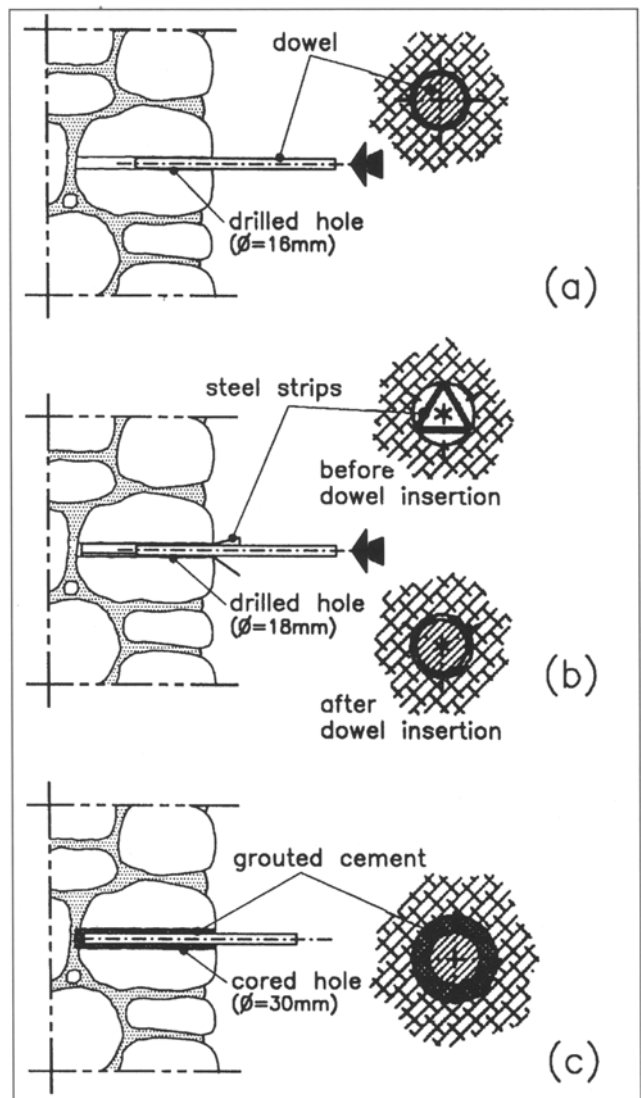


Fig. 1 – Dowel embedding techniques: a) rod forced in a calibrated hole (type A); b) rod forced in a hole interposing three steel strips (type B); c) rod embedded with cement grout (type C).

strips are positioned before forcing the rod inside [6], as shown in Fig. 1b.

The third technique (type C) adopts a greater hole diameter (30 mm), made with the corer, and the steel rod is embedded injecting a tixotropic cement grout (Fig. 1c).

As pointed out in the preceding tests [6], the shear load applied to the wall by the dowel connector influences in a significant way only a limited zone close to the loaded masonry unit. For this reason, the test specimens were made with a few common cobblestones (average size 15-20 cm) assembled in one layer (20 cm thick) and forming a rectangular masonry element (43 x 48 cm), as illustrated in Fig. 2. A reinforced concrete frame has been utilised to simulate the confinement of the surrounding masonry.

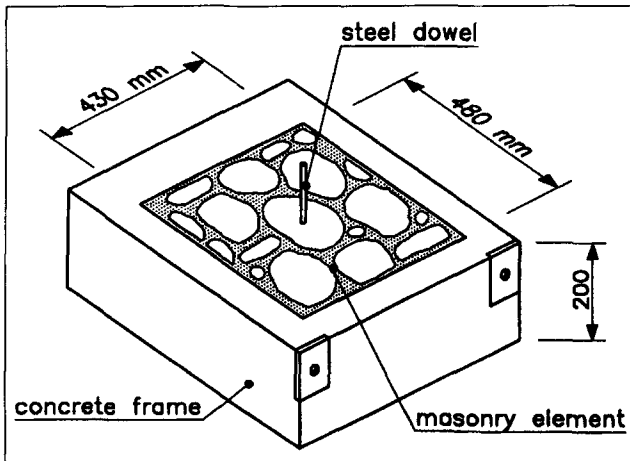


Fig. 2 – Isometric view of the test specimen.

The kind of rock in the loaded stone block of each specimen as well as the compressive strength, evaluated on prisms (3 x 3 x 6 cm), are reported in Table 1.

The mortar used to bind the stone blocks was made with silica sand and hydraulic lime. This kind of binder has been preferred to the hydrated lime in order to obtain a homogeneous curing within a reasonable period of time. The hydraulic lime dosage has been chosen in order to obtain the same resistance to penetration as in the masonry mortar of the ancient building where tests [6] were performed. The penetration test, which was set up to evaluate the wood decay in timber structures [10], gives indications about mechanical characteristics of the mortar according to some early experiments in progress. The test allows checking the resistance of the material to the gradual penetration of a conical-nosed steel probe which advances by means of repeated blows of a standard rebound hammer (impact energy: 2.2 J). The main characteristics of the mortar are summarised in Table 2.

During the set-up of the specimen, particular care was taken to make the specimen surface perfectly flat and smooth, as requested for the geometric interferometry technique. In fact, the stripping grating has to be glued onto the specimen surface, and the reference grating has to adhere to the former by means of a film of paraffin oil, in order to avoid interference losses or distortions.

For this purpose, a small cap was preliminarily cut from all the cobblestones so as to obtain a flat face with an average dimension of about 3/4 of the stone's size. Furthermore, each central stone block, where the dowels had to be inserted, was drilled before cutting the cap so that possible hole-mouth irregularities could be avoided.

Then, the cobblestones were laid with their faces against the flat bottom of the formwork. The voids between the cobblestones were carefully filled with the mortar and, after a few days, the confining concrete frame was cast (Fig. 2). After curing, the specimens were overturned and the dowels were fastened into the holes using the three aforementioned techniques.

Two specimens for each kind of dowel anchorage were tested in the present work.

### 3. EXPERIMENTAL APPARATUS AND TEST PROCEDURE

The dowel connectors considered herein have to transfer the shear load between the concrete slab and the masonry wall. Nevertheless, the need for a broad visibility of the moiré gratings required replacing the concrete slab with an appropriate steel device (Figs. 3a, b).

The behaviour of the dowel in the concrete slab may be simulated by adjusting the geometrical parameters *e* and *b* (Fig. 3b) which were calibrated considering the stiffness and ultimate load of dowels embedded in the concrete according to the theoretical models available in the literature [11, 12]. In this way, the interlocking effect was neglected, in agreement with the aim of the present investigation.

The connection deformation can be described by three significant displacements, as illustrated in Fig. 3c. The global slip *s* includes the deformation of the dowel, both in the "concrete part" and in the stone block, and the displacement  $\eta_s$  of the stone block. The dowel displacement  $\eta_d$ , surveyed at the stone surface, represents

Table 1 – Characteristics of stone blocks

Specimen	Kind of rock	Compressive strength [MPa]
A1	Sandstone (graywacke)	88
A2	Sandstone	76
B1	Limestone (calcirudite)	113
B2	Sandstone (graywacke)	119
C1	Limestone (biorudite)	156
C2	Microfractured dolomite	47

Table 2 – Characteristics of mortar

Maximum size of sand	5 mm
Hydraulic lime binder dosage	140 kg/m <sup>3</sup>
Water-lime ratio	0.68
Average compressive cylindrical strength (90 days)	0.71 MPa
Elastic modulus	3000 MPa
Penetration resistance according to Ref. 10	5 hit/cm

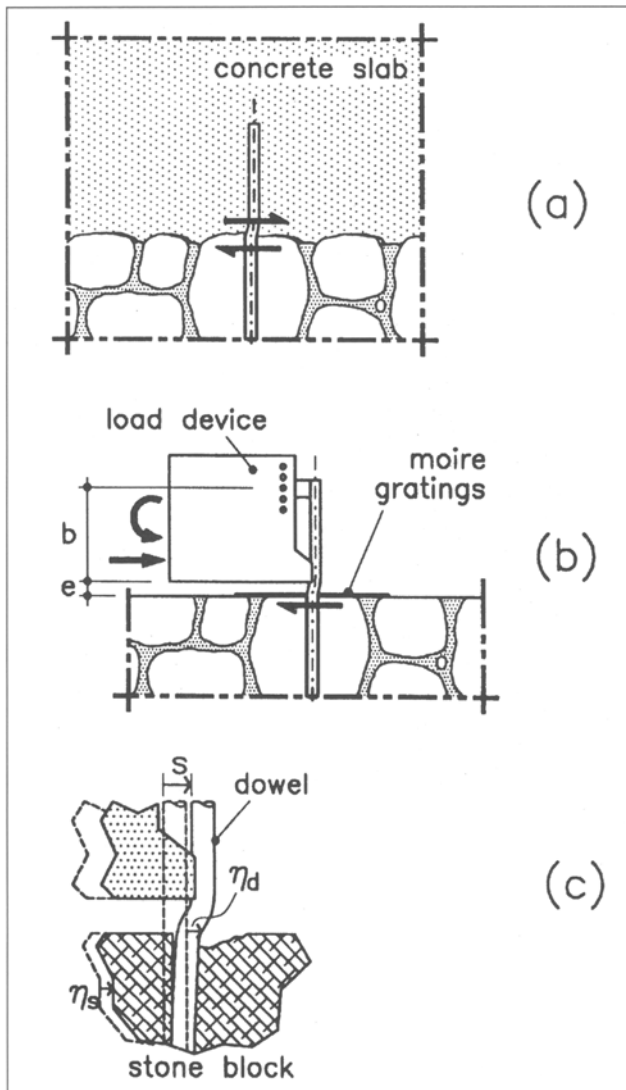


Fig. 3 - a) actual concrete slab-to-masonry connection; b) simulation of concrete slab with a steel device; c) displacements in the load direction.

the most significant displacement of the dowel-stone block system. The difference  $s - \eta_d$  depends mainly on characteristics of the concrete slab and does not concern the present research.

In Fig. 4, each part of the experimental apparatus is shown in detail. The steel frame (b) permits the load device (a) to move parallel to the specimen surface. In fact, two pairs of steel bars (c) connect the frame (b) to the concrete bench (d), where the concrete frame of the specimen has been horizontally laid interposing a thin mortar layer (e). Two notches have been machined at each end of the steel bars (c), in order to form the plastic hinges that allow the steel frame to slip without any clearance.

The reaction arrangement (f) is restrained to the concrete frame of the specimen by means of two threaded tendons (g). The load is applied between the steel device (a) and the reaction arrangement (f). In this way, the applied forces constitute a self-equilibrated system with the specimen (thick black arrows in Fig. 4).

The load machine (h) is the same employed in previous experimental tests [6] and is based on a lever system.

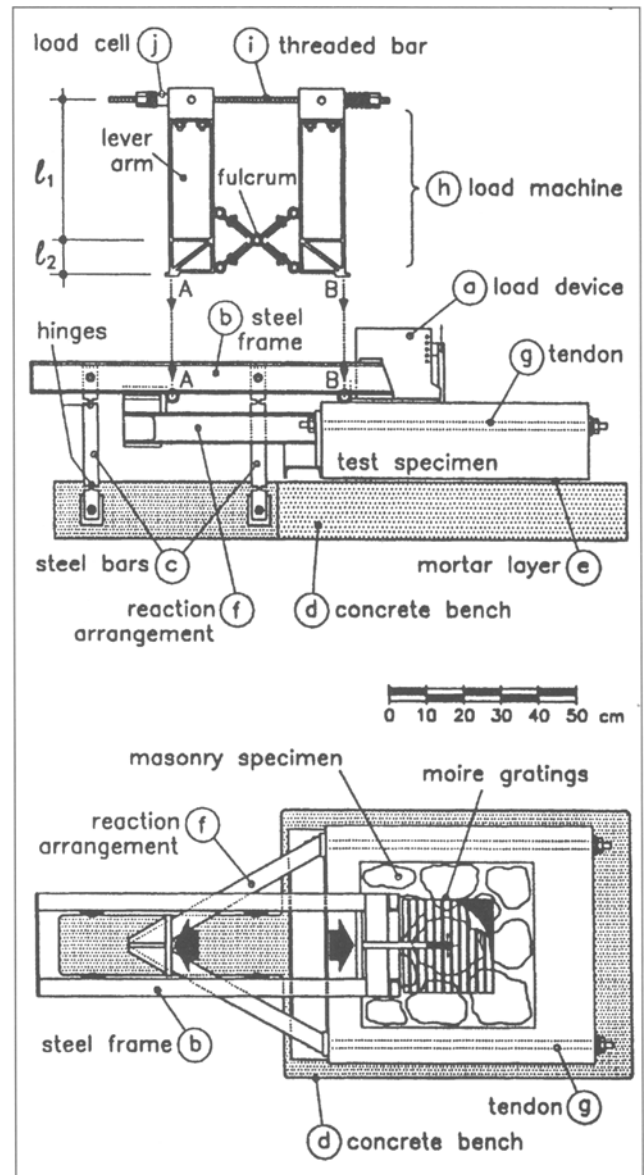


Fig. 4 - Frontal view and plan of the experimental apparatus.

The force obtained in screwing the threaded bar (i) is measured with the load cell (j) and amplified by a load factor that depends on the lever arm ratio  $l_1/l_2$ . The load obtained corresponds to the shear force actually applied to the dowel.

As already mentioned, the surface displacements around the dowel have been measured by means of the geometric interferometry technique (Fig. 5). In this manner, it was even possible to evaluate the stone block displacement  $\eta_s$ . The stripping grating (a) (pitch 0.025 mm) is glued in the center of the specimen with the lines orthogonal to the load direction. The reference grating (a') (same pitch) is superimposed onto the stripping fixing at two points (P,P') of its frontal edge to the masonry surface.

In order to refer all the horizontal displacement measures to the same reference (steel plate (b) on the rear of the specimen), the position of the above points has to be surveyed during the test. Hence, two electrical gauges (c) are fixed in P,P' while two steel wires (d), kept in

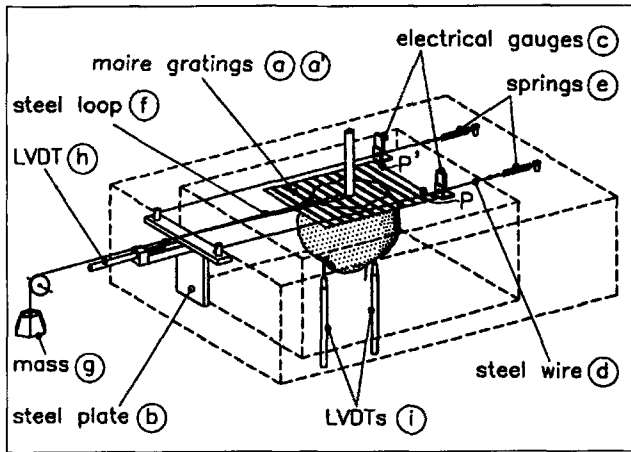


Fig. 5 - Arrangement of electrical gauges and moiré gratings.

tension with steel springs (e), link the sensing heads of the gauges to the reference plate (b). The steel loop (f) girdles the dowel close to the specimen surface, thereby allowing capturing the dowel displacement  $\eta_d$  on the ideal concrete slab-masonry interface. The mass (g) keeps the wire tension constant while an inductive transducer (h) measures the displacement  $\eta_d$ . Two other inductive transducers (not shown in the figure) are fixed to the reference plate (b) by means of magnetic supports and allow gauging the load device slip  $s$ . This slip actually simulates the global displacement (Fig. 3) between masonry wall and concrete slab.

Furthermore, the vertical translation and the rotation of the central stone block in the load plane are obtained

from the measures given by the inductive transducers (i). They are fixed to the confining concrete frame, and their heads reach two grinded small plates by passing through plastic pipes embedded in the mortar of the specimen.

The tests were carried out by increasing, step by step, the slip of the load device (average slip rate 0.005 mm/s). Increments of 0.1 mm were imposed up to a total slip of about 2 mm, while increments of 0.2 mm were adopted for higher slip values. At each loading step, the next slip increment was applied once the shear load had been stabilized (*i.e.* rate of load variation almost 1/10 of the initial value).

At the end of each loading step, the measures given by the gauges were recorded and a photograph of the moiré fringes was taken.

#### 4. RESULTS

Besides the load-slip relationship of the connection, each test provided a sequence of images showing the field of the stone surface displacements around the dowel. As a matter of fact, the fringe pattern at each loading step makes the evaluation of the displacements in the direction of the load possible. Moreover, the main phenomena occurring in the stone block can be surveyed through the images of fringes at each step. In Figs. 6 and 7, the fringe pattern of some significant loading steps are reported for test specimens B1 and C2, respectively.

In each picture, the values of the corresponding load  $F$  and load device slip  $s$  are typed in the zone at the left of

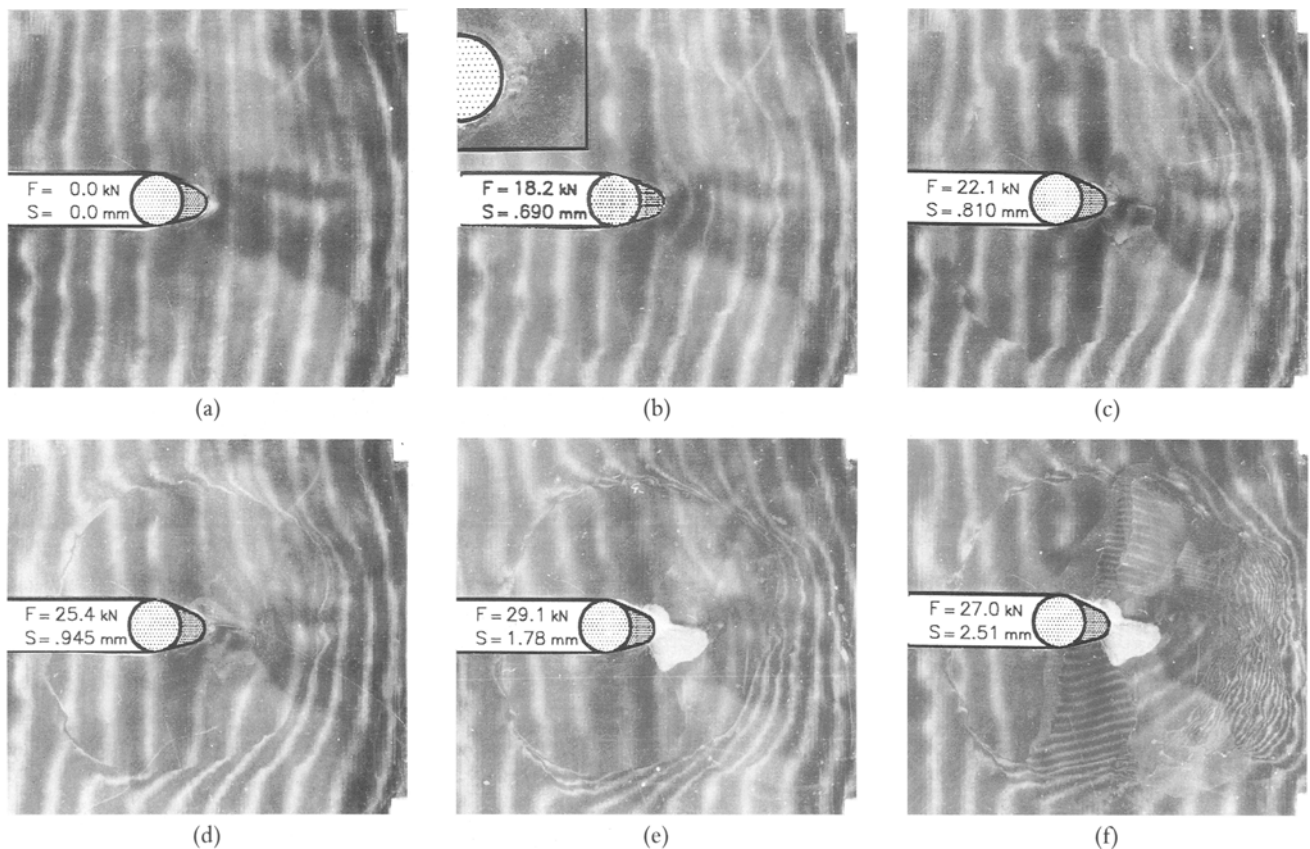


Fig. 6 - Sequence of fringe pattern for test specimen B1.

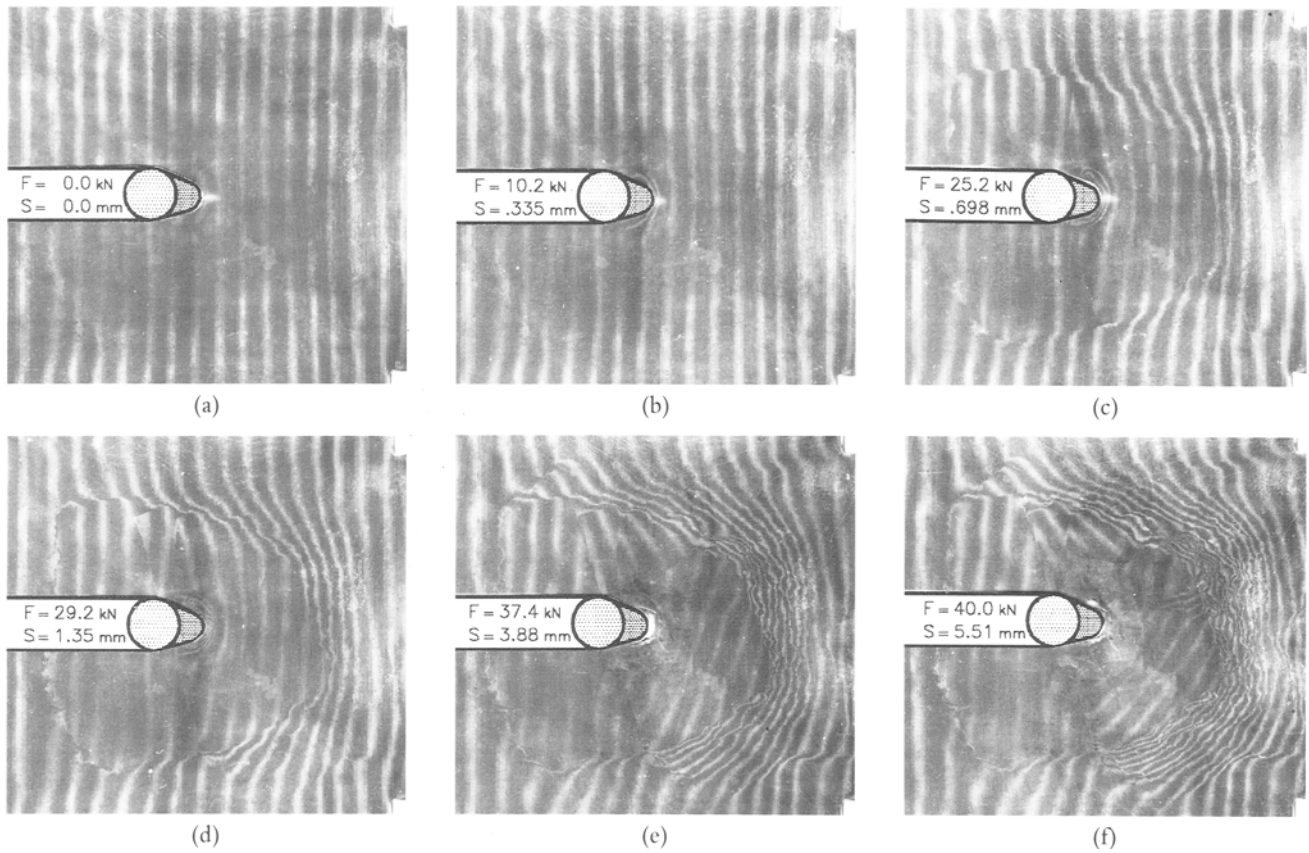


Fig. 7 – Sequence of fringe pattern for test specimen C2.

the dowel where fringes are hidden by the loading device (a) of Fig. 4. The fringe image concerns the area of the loaded stone block and part of the surrounding masonry. Fig. 6d-f and Fig. 7c-f show the stone boundary as revealed by the localised deformation of fringes due to the relative displacements between loaded stone block and surrounding masonry.

The distortion of fringes in front of the dowel, as shown in Figs 6b and 6c, highlights the gradual formation of a conical splinter accompanied by some radial microcracks very close to the bar (detail at top left of Fig. 6b). This kind of damage has been observed in all specimens in which the steel rod is embedded in the stone block without any gluing material (test groups A and B). As the load increases, the splinter tends to uplift and causes the lack of interference between gratings. Its removal was therefore needed in order to restore the contact between gratings and then proceed with the test (Figs. 6d and 6e).

The stone block damage continues with the formation of some radial cracks that gradually reach the mortar joint (Fig. 6e). Afterwards, a sudden global splitting occurred that greatly increased the crushing of the mortar layer in front of the stone block (Fig. 6f) as demonstrated by the extreme closeness of the fringes.

The same behaviour has also been observed in fringes of tests A2 and B2, herein not included, but no sudden block failure occurred in the former because of the effective confinement provided by the stones surrounding the loaded one and bound with thin mortar joints. Only two capillary cracks were noted in specimen A1.

A different behaviour characterises the initial loading steps of test C2. In fact, the local deformations close to the dowel are concentrated in the cement grout surrounding the bar, and no conical splinters appeared even though this kind of rock includes various small weak layers (Figs. 7b and 7c). For the previous reason, the formation of the splitting cracks (Fig. 7c) and their ensuing propagation (Figs. 7d, 7e and 7f) were not delayed as expected. On the contrary, the stone block of specimen C1, made with a strong kind of rock (see Table 1), did not split at all, but only a large splinter was detached when the slip reached a rather high value (*i.e.* 6.59 mm). The damage surveyed at the end of each test is reported in Fig. 8.

Fig. 9 shows the curves of load versus dowel displacement  $\eta_d$  for the three couples of specimens. The detachment of conical splinters is indicated with circle marks. Square marks point out that the splitting crack has reached the edge of the stone. Moreover, triangles are used to show the sudden formation of the global splitting that usually involves a significant drop of connection-bearing capacity.

For each specimen, the experimental curve shows a high ductility of the connection. In the figures, the curves are plotted for up to 5 mm of the dowel displacement  $\eta_d$ , because greater values have no practical sense, and no significant decreases of the load were evaluated. All curves initially show an almost linear branch whose beginning is made softer by possible clearances between the rod and the stone hole. This effect is more pronounced in anchorage technique B, whereas it is absent in anchorage technique C. The slopes of the curves display a sudden change for

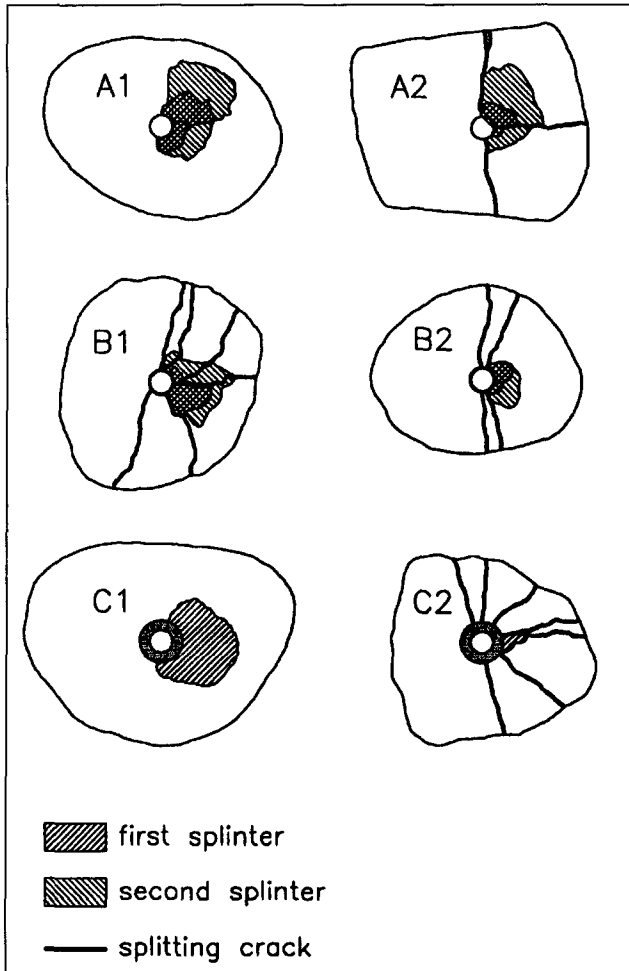


Fig. 8 - Damage in the loaded stone blocks at the end of testing.

load values which is quite close even though they refer to different embedding techniques of the dowels.

In Fig. 10, the load versus block displacements  $\eta_s$  for each specimen is plotted. These curves have been obtained from moiré fringes. The last point of each curve (asterisk) indicates the lack of interference between gratings because the stone surface does not remain plane for a long time after splitting.

The contribution of block displacement  $\eta_s$  is usually small when compared with dowel displacement  $\eta_d$  and their ratio  $\eta_s/\eta_d$  ranges from 1/20 for specimen A1 to 1/2 for specimen B1.

Fig. 11 compares the curves of load versus dowel displacement  $\eta_d$  and of load versus global slip  $s$  for specimen A1. For a given load, the dowel displacement value is approximately 50% of the global slip value. The same results have been noted for the other specimens tested, as can be shown by the almost linear slopes of the curves of Fig. 12. Appreciable changes in the curves are due to the splitting of the stone blocks which causes an increment in the ratio between the dowel displacement  $\eta_d$  and the global slip  $s$ .

The curves plotted in Figs. 13a and 13b refer to the same images of tests B1 and C2, respectively, as discussed above (Figs 6 and 7), and give the surface displacements measured with the moiré technique along the loading axis  $x$ .

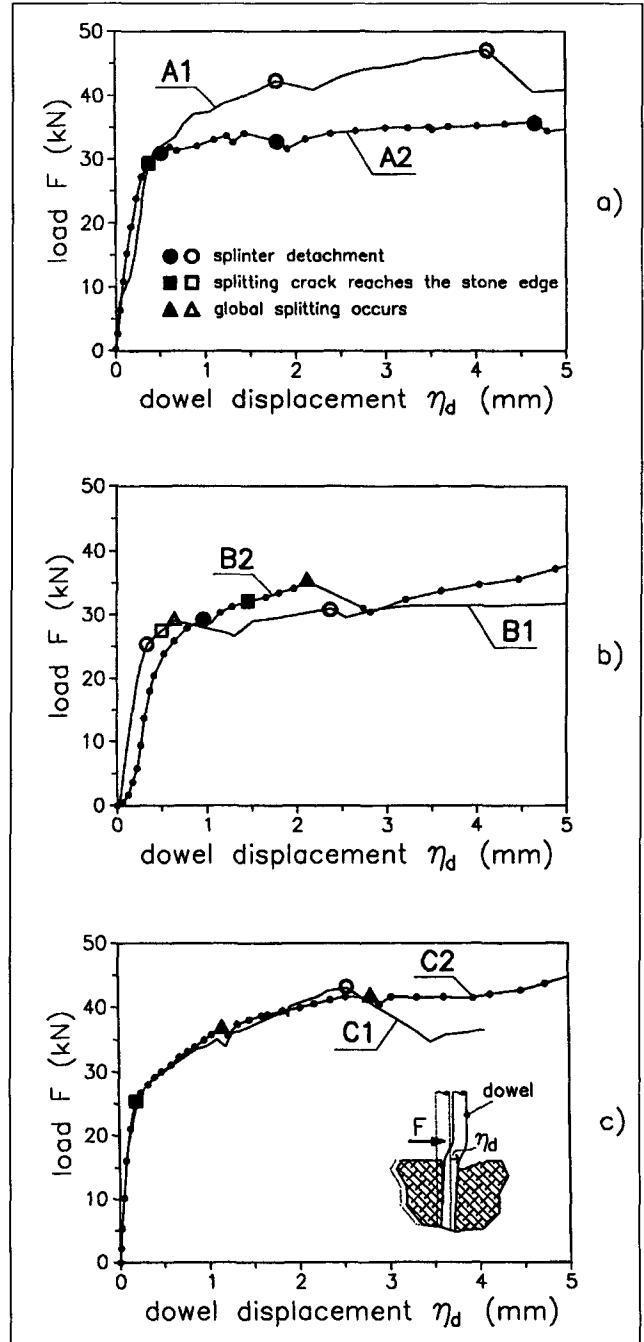


Fig. 9 - Shear load/dowel displacement relationship for the three embedding techniques considered.

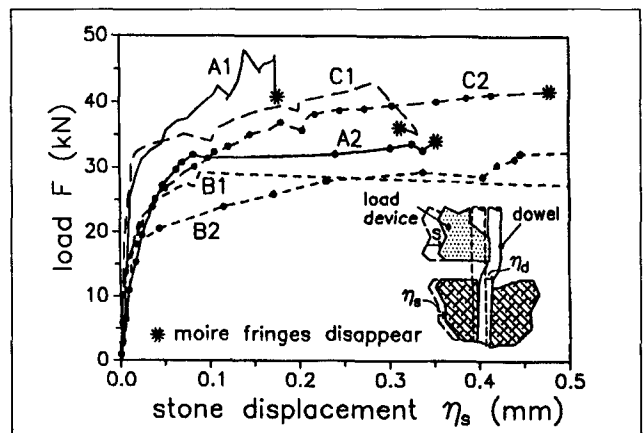


Fig. 10 - Shear load/stone displacement relationships for specimens tested.



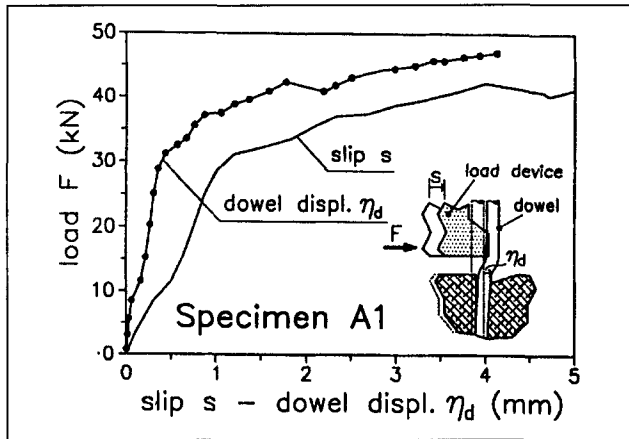


Fig. 11 - Shear load/slip and shear load/dowel displacement relationships for specimen A1.

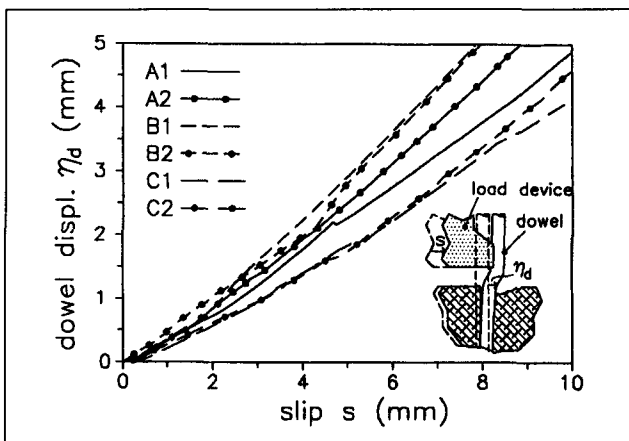


Fig. 12 - Relationship between dowel displacement and loading device.

For each loading step, the flat branches of these curves both in front and behind the dowel show the stone block translation. During the progress of the test, an increasing discontinuity between the displacements of the frontal and rear part of the stone block can be noted. This gap is due to the splitting crack opening and becomes dramatically evident when the global splitting is reached (arrows in Fig. 13a).

The local deformations in the stone block close to the dowel are not clearly valuable with the moiré technique because of the splinter formation (Fig. 13a). Therefore, the dashed part of the curves has not actually been surveyed, but they connect the frontal branches to the points (circles) corresponding to the dowel displacement  $\eta_d$  measured with the steel loop (f) of Fig. 5. The peak of the curves in front of the dowel is due to the detachment of the splinter.

In test specimens that adopt the injecting connection technique, the absence of splinters allows measuring the local displacements close to the bar (Fig. 13b). The greatest part of the local deformation is concentrated in the grouted cement layer where plastic flow is possible.

The stone block displacement  $\eta_s$  of Fig. 10 has been obtained measuring the displacements of Fig. 13 on the stone edge A.

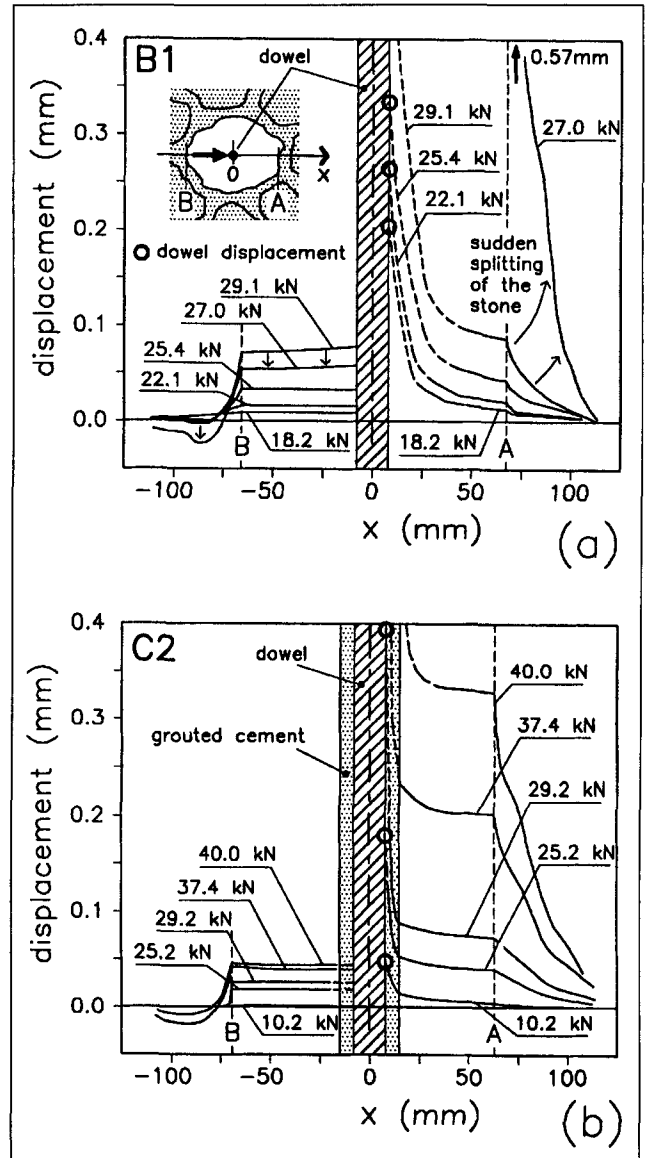


Fig. 13 - Surface displacements surveyed with the moiré technique for a) test specimen B1 and b) test specimen C2.

## 5. CONCLUDING REMARKS

The results of an experimental investigation on the behaviour of steel dowel connections used to transfer horizontal shear forces between concrete slabs and stone masonry walls have been presented herein.

The purpose of this research was to study the connection deformation in the masonry wall. The moiré interferometry technique allowed capturing the local effects of both the shear load on the surface of stone blocks and the mortar joints.

The results obtained enable outlining the following concluding remarks.

- The initial stiffness can be affected by the clearances between the dowel and the stone block hole when anchorage techniques without any gluing material are adopted.
- The three examined embedding techniques of dowels in the stone block do not show appreciable differences in the bearing capacity of the connection.



- The connections are characterised by a remarkable ductility. In fact, the bearing capacity is maintained up to very large displacements (beyond 5 mm - Fig. 9).
- The stone block splitting and the splinter formation in front of the dowel do not provoke a sudden and relevant drop in bearing capacity.
- The displacement of the almost-rounded stone block considered (about 15 cm in size) was quite small in comparison with that of the dowel (Fig. 10), and the majority of this displacement is due to the crushing of the mortar in the joint against which the loaded stone block is forced.

These early results provide some knowledge of the local phenomena regarding a steel dowel embedded in a stone masonry wall, but they are not exhaustive due to the limited number of tests. Other kinds of stones, as well as different mortar grades, should be considered for testing in further research work.

## 6. ACKNOWLEDGEMENTS

The financial support of the Italian Ministry of University and Scientific Research (MURST) is gratefully acknowledged.

## REFERENCES

- [1] Benedetti, D., 'Reparation and strengthening of masonry buildings', in 'Costruzioni in Zona Sismica' (Masson Italia Editore, Milan, 1981) 327-398 (in Italian).
- [2] Giuriani, E., Ronca, P., Noro, P. and Veroli, M., 'Early experimental results on wood-concrete floors subjected to seismic action' (in Italian), Atti del 5° Convegno Nazionale L'Ingegneria Sismica in Italia, 29.09-2.10.1991, Palermo, Italian National Association for Earthquake Engineering.
- [3] Ronca, P., Gelfi, P. and Giuriani, E., 'The behaviour of a wood-concrete composite beam under cyclic and long term loads', in Proceedings of STREMA (Structural Repair and Maintenance of Historical Buildings), Seville, 1991, 264-275.
- [4] Castellani, A., Ruggeri, L., Boffi, G. and Cenon, F., 'Strengthening of masonry buildings: effectiveness of connections between floors and walls concerning the redistribution of horizontal forces', (in Italian), *Ingegneria Sismica* Anno VI (No. 1) (1989) 49-61.
- [5] Sanders, H. P., 'A case history - retrofit seismic strengthening of John Marshall High School with historic restoration objectives', in Proceedings of the 8th World Conference on Earthquake Engineering, San Francisco, 1984, 617-624.
- [6] Giuriani, E., Gattesco, N. and Del Piccolo, M., 'Experimental tests on the shear behaviour of dowels connecting concrete slabs to stone masonry walls', *Mater. Struct.* **26** (1993) 293-301.
- [7] Giuriani, E. and Ronca, P., 'The crack pattern in an R.C. beam analyzed by means of the optical interferometry' (in Italian), Atti VII Convegno Nazionale AIAS, Cagliari, Sept. 1979, 6.1-6.15.
- [8] Tassios, T.P., and Koroneas, E.G., 'Local bond-slip relationships by means of the moiré method', *ACI Journal, Proc.* **81** (Jan-Feb. 1984) 27-34.
- [9] Biolzi, L and Giuriani, E., 'Bearing capacity of a bar under transversal loads', *Mater. Struct.* **23** (1990) 449-456.
- [10] Giuriani, E. and Gubana, A., 'Penetration test to evaluate wood decay and its application to the loggia monument', *Mater. Struct.* **26** (1993) 8-14.
- [11] Dulacska, H., 'Dowel action of reinforcement crossing cracks in concrete', *ACI Journal* **69** (12) (1972) 754-757.
- [12] Vintzeleou, E.N. and Tassios, T.P., 'Mathematical models for dowel action under monotonic and cyclic conditions', *Magazine of Concrete Research* **38** (134) (1986) 13-22.